JACS
JOURNAL OF THE AMERICAN CHEMICAL SOCIETY
pubs.acs.org/JACS
Article

Bioorthogonal Photocatalytic Decaging-Enabled Mitochondrial Proteomics

Zongyu Huang,[#] Ziqi Liu,[#] Xiao Xie, Ruxin Zeng, Zujie Chen, Linghao Kong, Xinyuan Fan,* and Peng R. Chen*

Cite This: https://doi.org/10.1021/jacs.1c09171
Read Online

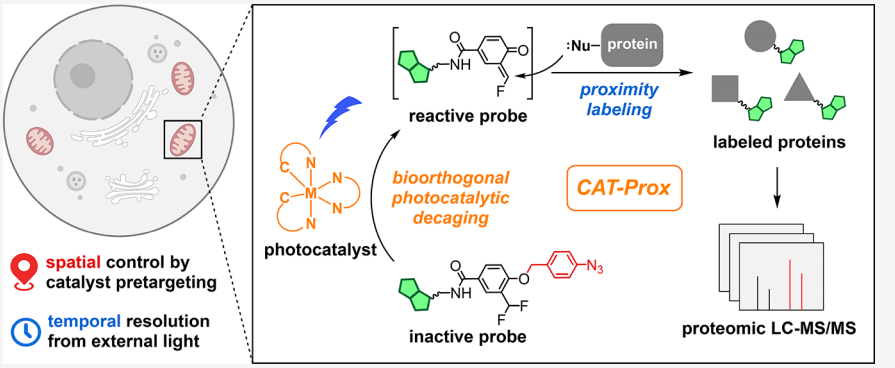

ABSTRACT: Spatiotemporally resolved dissection of subcellular proteome is crucial to our understanding of cellular functions in health and disease. We herein report a bioorthogonal and photocatalytic decaging-enabled proximity labeling strategy (CAT-Prox) for spatiotemporally resolved mitochondrial proteome profiling in living cells. Our systematic survey of the photocatalysts has led to the identification of $Ir(ppy)_2bpy$ as a bioorthogonal and mitochondria-targeting catalyst that allowed photocontrolled, rapid rescue of azidobenzyl-caged quinone methide as a highly reactive Michael acceptor for proximity-based protein labeling in mitochondria of live cells. Upon careful validation through *in vitro* labeling, mitochondria-targeting specificity, *in situ* catalytic activity as well as protein tagging, we applied CAT-Prox for mitochondria proteome profiling in living Hela cells as well as hard-to-transfect macrophage RAW264.7 cells with approximately 70% mitochondria specificity observed from up to 300 proteins enriched. Finally, CAT-Prox was further applied to the dynamic dissection of mitochondria proteome of macrophage cells upon lipopolysaccharide stimulation. By integrating photocatalytic decaging chemistry with proximity-based protein labeling, CAT-Prox offers a general, catalytic, and nongenetic alternative to the enzyme-based proximity labeling strategies for diverse live cell settings.

INTRODUCTION

The spatiotemporally organized subcellular proteome (e.g., protein abundance, turnover rates, interactions, post-translational modifications) is fundamental to virtually all life processes.[1,2] For example, as the powerhouse of cells, the dynamic proteome in mitochondria plays crucial roles in maintaining cellular processes such as energy and redox homeostasis.[3] Perturbation of mitochondrial proteome homeostasis has been linked to many human diseases such as cancer, metabolic disease, and neurodegenerative disorders.[4] As a result, dissection of the mitochondria proteome of different cell types, especially in a spatiotemporally resolved manner, may facilitate the mechanistic elucidation of biological processes as well as human diseases.[5] Conventional approaches require isolation of mitochondria after cell lysis, which suffers from low temporal resolution and possible contamination with other subcellular compartments.[6] Enzyme-mediated proximity labeling (e.g., APEX, TurboID) have been developed for mitochondria proteome enrichment via *in situ* generated reactive chemical species (e.g., phenol radical or biotinylating intermediate).[7,8] However, such methods are largely affected by the property of the fusion bait protein that may have multiple or altered subcellular locations when overexpressed inside cells.[2] Furthermore, the gene transfection procedures rendered these methods difficult for hard-to-transfect cells (e.g., macrophage cells), primary neuron, or tissue samples. The recently reported chemical probe-based approaches coupled the mitochondria-targeting group with reactive species for mitochondria proteome profiling in primary neuron cells

Received: August 30, 2021

(e.g., ORMs), which had potential advantages by avoiding genetic operations.[9,10] However, the direct usage of reactive probes might cause off-labeling given the potent reactivities when passing through the cellular membrane and cytosolic space. Alternative chemical approaches have also emerged lately, including the micromapping of protein network by photocatalytic generation of carbene species via Dexter energy transfer.[11] But the intracellular labeling of the whole proteome is still challenging for such short-ranged carbene species.

Given the urgent query of mitochondria proteome dynamics in diverse living settings,[4] we envisioned that a general platform that integrates the advantages of both enzymatic and chemical approaches is highly desirable, which would ideally fulfill: (i) *in situ* generation of reactive species in mitochondria to avoid plausible off-labeling, (ii) catalytic activation of reactive species in a similar fashion as the enzymatic approaches, (iii) straightforward and nongenetic operations for diverse cell types or tissue samples that is similar to the chemical approaches, (iv) capability for noninvasive and remote-control with high temporal resolution, and (v) modular and programmable design with broad applicability.

We herein report a bioorthogonal photocatalytic decaging chemistry-based spatiotemporal proteomics strategy (CAT-Prox) in living cells. Systematic surveys of bioorthogonal photocatalysts have enabled us to identify an iridium photocatalyst for rapid decaging of *para*-azidobenzyl protection group (PAB), allowing photocontrolled *in situ* release of highly reactive quinone methide intermediates for proteome profiling. We applied this CAT-Prox strategy for the dynamic dissection of mitochondria proteomes of cancer cells as well as hard-to-transfect macrophage cells upon lipopolysaccharide (LPS)-stimulated inflammation (Scheme 1).

Scheme 1. Schematic Illustration of the CAT-Prox Strategy and the Workflow of Subcellular Proteomics

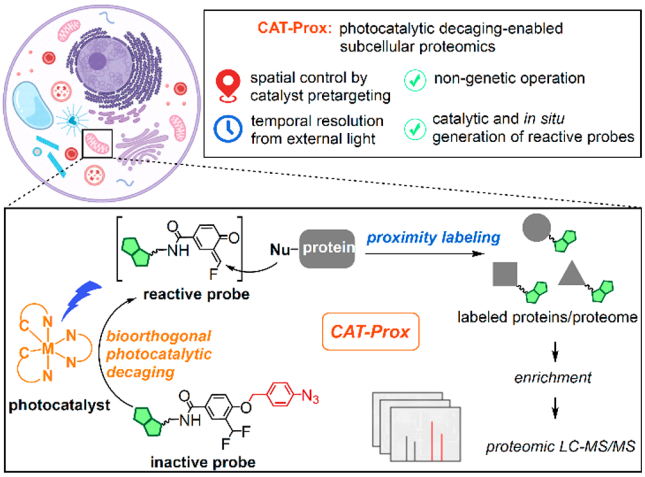

RESULTS AND DISCUSSION

We started by developing the bioorthogonal decaging chemistry[12−14] with major considerations on modifiable catalysts for spatial targeting to mitochondria, external visible light for temporal regulation, and fast reaction kinetics for precise temporal control. The transformation of aryl azide to aniline was chosen as the model reaction due to its well-documented bioorthogonality, but further development of more suitable catalytic system is needed for expanding the utility of this reaction in living systems.[14−16] Therefore, 4-azidobenzoic acid (**1**) was subjected to a collection of photocatalysts (10 mol %), including ruthenium complexes, organic photosensitizers, and iridium complexes, under white LED irradiation in H_2O/DMSO (1/1) with NADH as additive (Figures 1a and S1). The reaction was monitored using HPLC for 30 min. While low to moderate conversions were observed with the commonly used ruthenium complexes and organic photosensitizers, the iridium complexes showed very high catalytic activities.[17−19] In particular, full conversion was obtained with $[Ir(2',4'\text{-}F_2\text{-}5\text{-}CF_3\text{-}ppy)_2(bpy)]PF_6$ (**Ir7**). Next, the catalyst analogue **Ir8** with *t*Bu substituents on the C4 of bipyridine ligand was tested. Full conversion was observed as well, indicating the negligible effect of alkyl group introduction, which ensured the subsequent conjugation of targeting group from C4 position (Figure 1a). To further improve the reaction rate, blue LED light (λ_{max} = 450 nm, 4 mW/cm^2) was tested, and the reaction was monitored using HPLC (Figure S2). Consumption of **1** along with the appearance of **2** was rapidly observed, with the conversion completed within 15 min. In addition, it was noted that the persistence of **Ir8** in the HPLC traces indicated the sustainability of the catalyst for the reaction, further facilitating its utility as enzyme mimic in living systems (Figure 1b). The cytotoxicity of **Ir8** was evaluated next. Delightfully, no cytotoxicity was observed up to 2.0 μM of **Ir8** under reaction conditions (Figure 1c), whereas <0.2 μM of the catalyst was sufficiently enough in the following applications inside cells, which was far below the safe concentration, guaranteeing the biocompatibility of the decaging reaction in living cells.

With the efficient photocatalyzed bioorthogonal decaging reaction in hand, we next aimed to design controllable reactive probes for protein labeling. Although liberating highly reactive intermediates by decaging chemistry is highly challenging, we reasoned that quinone methide[20−22] is a very unique species that can be caged by masking its phenolic group until photocatalytic decaging-triggered rescue of the highly reactive Michael acceptor for covalent labeling with protein side-chains (e.g., Lys, Ser, Glu, Gln, Asp, Asn, and Arg).[21] To this end, we designed and synthesized a PAB-caged quinone methide probe (PAB-QM-Bio) tethered with a biotin handle (Figure 1d), which could be transformed into a reactive quinone methide intermediate in response to our photocatalytic decaging reaction to label neighbor proteins. Thus, the labeled proteins could be further purified based on biotin−streptavidin enrichment. The decaging efficiency was first tested in aqueous solution. Complete conversion of PAB-QM-Bio into 2-hydroxybenzaldehyde species, the product of cascade hydrolysis of the decaged quinone methide intermediate, was obtained within 15 min in the presence of both **Ir8** (10 mol %) and blue LED irradiation (Figure 1e). The labeling efficiency of the PAB-QM-Bio probe was next evaluated using bovine serum albumin (BSA) (Figure 1f). Increased labeling intensity was observed along with the increasing of **Ir8** concentration, underlying the spatial specificity of protein labeling from the catalyst inside cells (Figure 1g). Pulse-chase labeling of proteins was verified by switching of photostimuli, revealing the temporal specificity from the external light (Figures 1h and S4). Together, a bioorthogonal photocatalytic decaging-enabled protein labeling system has been developed by integrating the unique advantages of photocatalytic chemistry and the high reactivity of decaging-triggerable quinone methide species.

https://doi.org/10.1021/jacs.1c09171
J. Am. Chem. Soc. XXXX, XXX, XXX−XXX

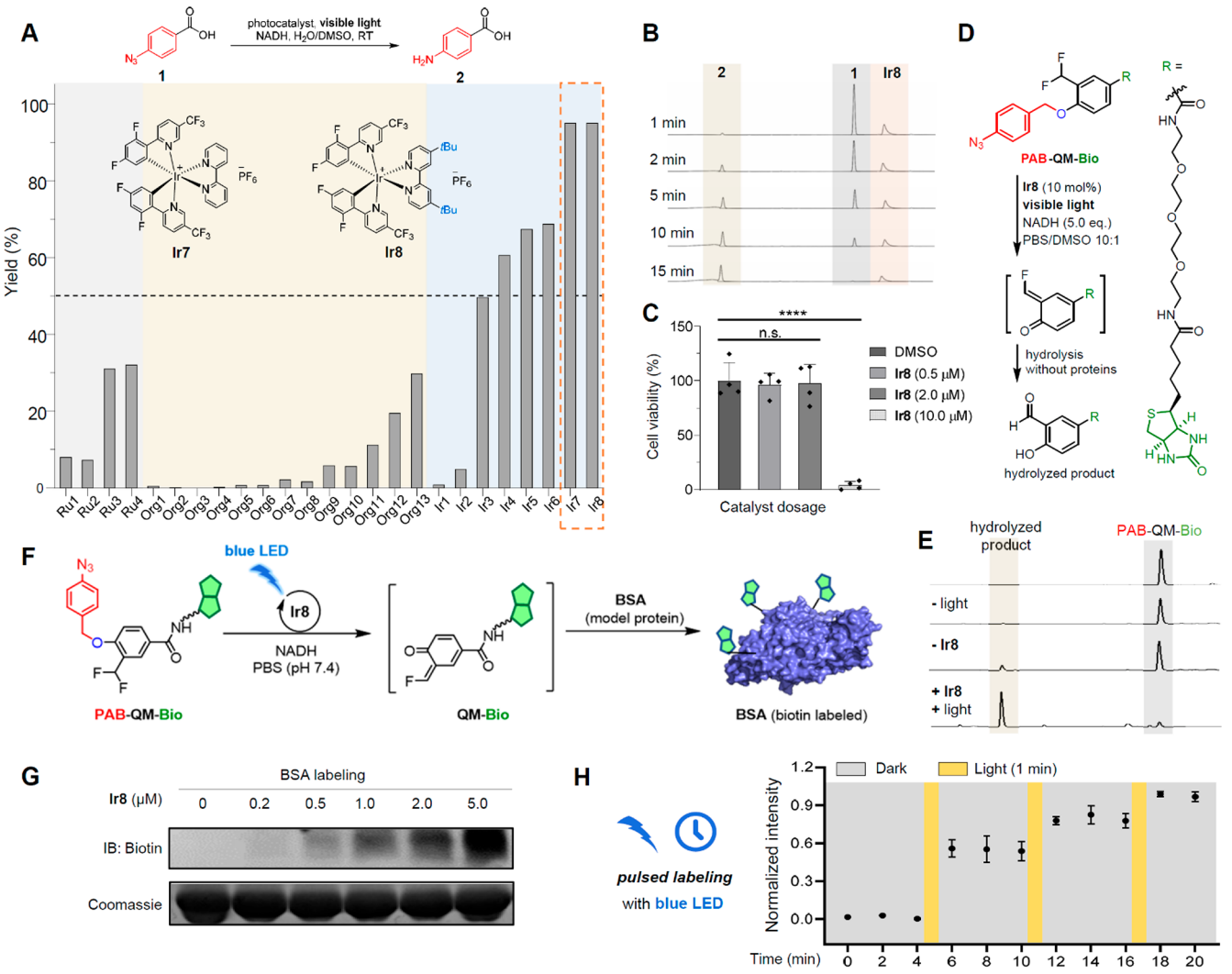

Figure 1. Development of the bioorthogonal and photocatalytic decaging-enabled proximity labeling strategy (Cat-Prox). (A) Catalyst screening for the aryl azide reduction reaction. The reaction was carried out with **1** (0.1 mmol) and NADH (0.2 mmol) in 0.5 mL mixture of water and DMSO (1/1) with photocatalyst (10 mol %, 0.01 mmol) at room temperature under white LED irradiation for 30 min. (B) HPLC traces of photocatalytic reduction of **1** under blue LED at given time points. Conditions: 0.1 mmol **1**, 0.2 mmol NADH, 10 mol % **Ir8**, in 0.5 mL water/DMSO (1/1), irradiated by mild blue LED (4 mW/cm^2). (C) Cytotoxicity evaluation of **Ir8**. (D) Design of quinone methide-based labeling probe (PAB-QM-Bio) and photocatalytic decaging of PAB-QM-Bio in aqueous media. (E) HPLC traces of the photocatalytic decaging of PAB-QM-Bio probe. Conditions: 0.1 mM PAB-QM-Bio, 0.5 mM NADH, 10 mol % **Ir8**, in PBS/DMSO (10/1) buffer, irradiated by blue LED (4 mW/cm^2) for 15 min. (F) *In vitro* evaluation of CAT-Prox using BSA as model protein. (G) Photocatalyst concentration-dependent labeling of BSA. Biotinylated BSA and total BSA were analyzed by immunoblotting and Coomassie blue staining, respectively. (H) Time-resolved BSA labeling by switching of the photostimuli.

We next aimed to target our photocatalyst into mitochondria (Figure 2a). Serendipitously, we discovered that **Ir8** itself was cell-membrane permeable and can gather at specific locations inside cells. Detailed analysis using confocal microscopy imaging with colocalization of MitoTracker Deep Red revealed that **Ir8** was localized in the mitochondria of all the cell lines we tested, most likely due to its positive charge and hydrophobic property (Figures 2b and S5). The Pearson's *R* value was determined to be 0.76 and 0.83 in HeLa and RAW264.7 cells, respectively, indicating the efficient targeting specificity of **Ir8** to mitochondria (Figure 2c). To verify the catalytic activity of **Ir8** in mitochondria, we synthesized PAB-caged rhodamine as the fluorogenic reporter, with the decaging-triggered conversion of PAB-rhodamine to rhodamine monitored by the rescued fluorescence (Figure 2d). We incubated HeLa cells with **Ir8** (200 nM) and MitoTracker Deep Red (100 nM) in culture media for 30 min. Noteworthy, 200 nM of **Ir8** was sufficient for the efficient photocatalytic decaging in living cells, most likely due to the higher local concentration of **Ir8** by its spontaneous accumulation in mitochondria. After washing, cells were charged with the PAB-rhodamine probe (50 μM) and irradiated under blue LED for 15 min. By confocal microscopy, we observed significant fluorescence of rescued rhodamine that colocalized with MitoTracker Deep Red, indicating the maintained catalytic activity of **Ir8** in mitochondria in living cells (Figure 2e,f).

With all the essential elements of CAT-Prox ready in hand, we next examined mitochondrial protein labeling in living cells (Figure 2g). Live HeLa cells were subjected to the CAT-Prox protocol, and immunofluorescence analysis was conducted subsequently. The colocalization of biotin immunofluorescence with mitochondrial marker TOMM20 indicated the *in*

https://doi.org/10.1021/jacs.1c09171
J. Am. Chem. Soc. XXXX, XXX, XXX−XXX

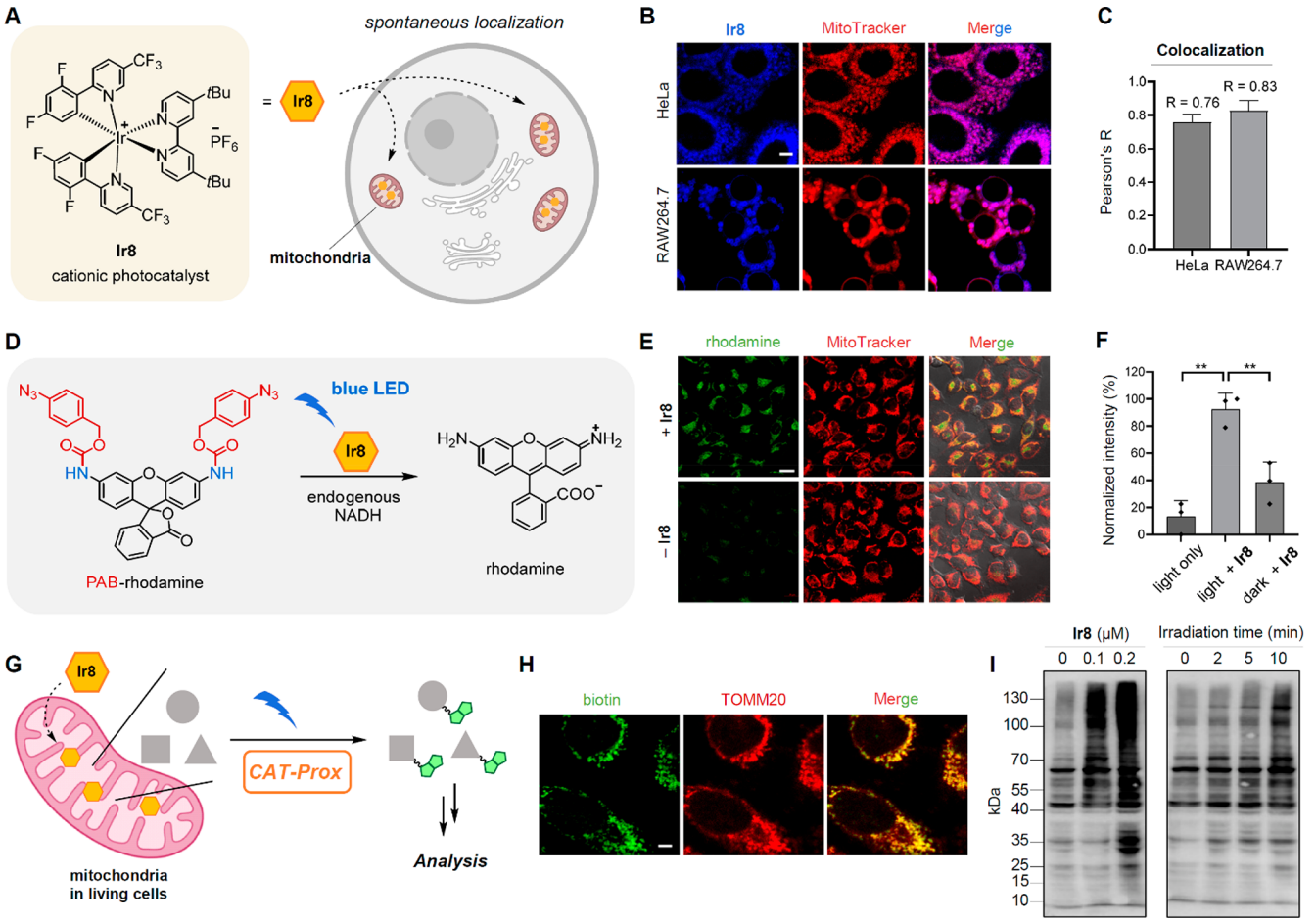

Figure 2. Development and validation of CAT-Prox as a catalytic and nongenetic strategy for mitochondria proteomics. (A) Targeting of **Ir8** photocatalyst into mitochondria via self-localization. (B) Confocal microscopic images of cells treated with **Ir8** (1 μM, blue) and MitoTracker Deep Red (100 nM, red). Scale bar, 5 μm. (C) Pearson's R value for evaluation of the colocalization in living cells. (D) Evaluation of **Ir8** catalytic activity by PAB-rhodamine decaging in mitochondria in living cells. (E) Confocal microscopic images showing the fluorescence of the rescued rhodamine 110. Scale bar, 20 μm. (F) Fluorescent quantification of the rescued rhodamine 110 in HeLa cells by flowcytometry. Data are represented as mean ± SD (n = 3 independent samples). $^{**}p < 0.0021$, unpaired two-tailed t-test. (G) Photocontrolled chemical proteomic profiling in mitochondria. (H) Immunofluorescence analysis of the HeLa cells after CAT-Prox labeling verified the *in situ* protein labeling in mitochondria. Scale bar, 5 μm. (I) Immunoblotting analysis of biotinylated proteins after CAT-Prox treatment of HeLa cells. Conditions: **Ir8** (0–200 nM), PAB-QM-biotin probe (100 μM), and blue LED irradiation (15 min) for the left gel; **Ir8** (100 nM), PAB-QM-biotin probe (100 μM), and blue LED irradiation (0–10 min) for the right gel.

situ labeling of proteins in mitochondria by CAT-Prox (Figure 2h). The protein labeling efficiency was evaluated by immunoblotting next. The mitochondria in live cells were charged with **Ir8** (ranging from 0 to 0.2 μM), followed by PAB-QM-Bio probe addition (100 μM) and blue LED irradiation up to10 min. After cell lysis, the biotinylated proteome was subjected to immunoblotting analysis which showed sufficient protein labeling with 0.2 μM catalyst loading and 10 min photoirradiation (Figure 2i).

By combining with the protein mass spectrometry, CAT-Prox would offer a powerful tool for mitochondria proteome profiling in living cells, which may facilitate the understanding of carcinogenic mechanism in cancer cells. To verify our method, we applied CAT-Prox to HeLa cells, and the biotin-labeled proteins were enriched with streptavidin-coated beads and analyzed by LC-MS/MS (Figure S6). Three independent experiments revealed 258 proteins with 182 mitochondria proteins identified according to MitoCarta3.0 database (70.5%) (Figure 3a). Submitochondrial analysis of the identified mitochondrial proteins revealed that the captured proteome maintained the original distribution profile (Figures 3a and S7a). This observation indicated CAT-prox could identify proteins from various subcompartmental regions of mitochondria. Moreover, with gene ontology (Biological Process) analysis powered by Metascape,[23] we noticed that the citric acid cycle (TCA)-related proteins were highly enriched from HeLa cells, consistent with the increased metabolic activities of cancer cells (Figure 3b).[24]

The mitochondrial proteome of immune cells can undergo highly dynamic regulation during immunological processes, including innate immune signaling as well as adaptive immune activation.[25] It is often challenging to dissect proteomes in immune cells by using enzymatic methods due to the natural defense to gene transfection of such cells.[26] We were interested in applying our CAT-Prox mitochondrial proteome profiling in macrophage cells by using RAW264.7 cells as the model. A total of 300 proteins were detected from three independent CAT-Prox experiments, with 216 mitochondrial proteins identified (72% specificity), demonstrating the high efficiency of CAT-Prox for mitochondrial proteome profiling in macro-

https://doi.org/10.1021/jacs.1c09171
J. Am. Chem. Soc. XXXX, XXX, XXX–XXX

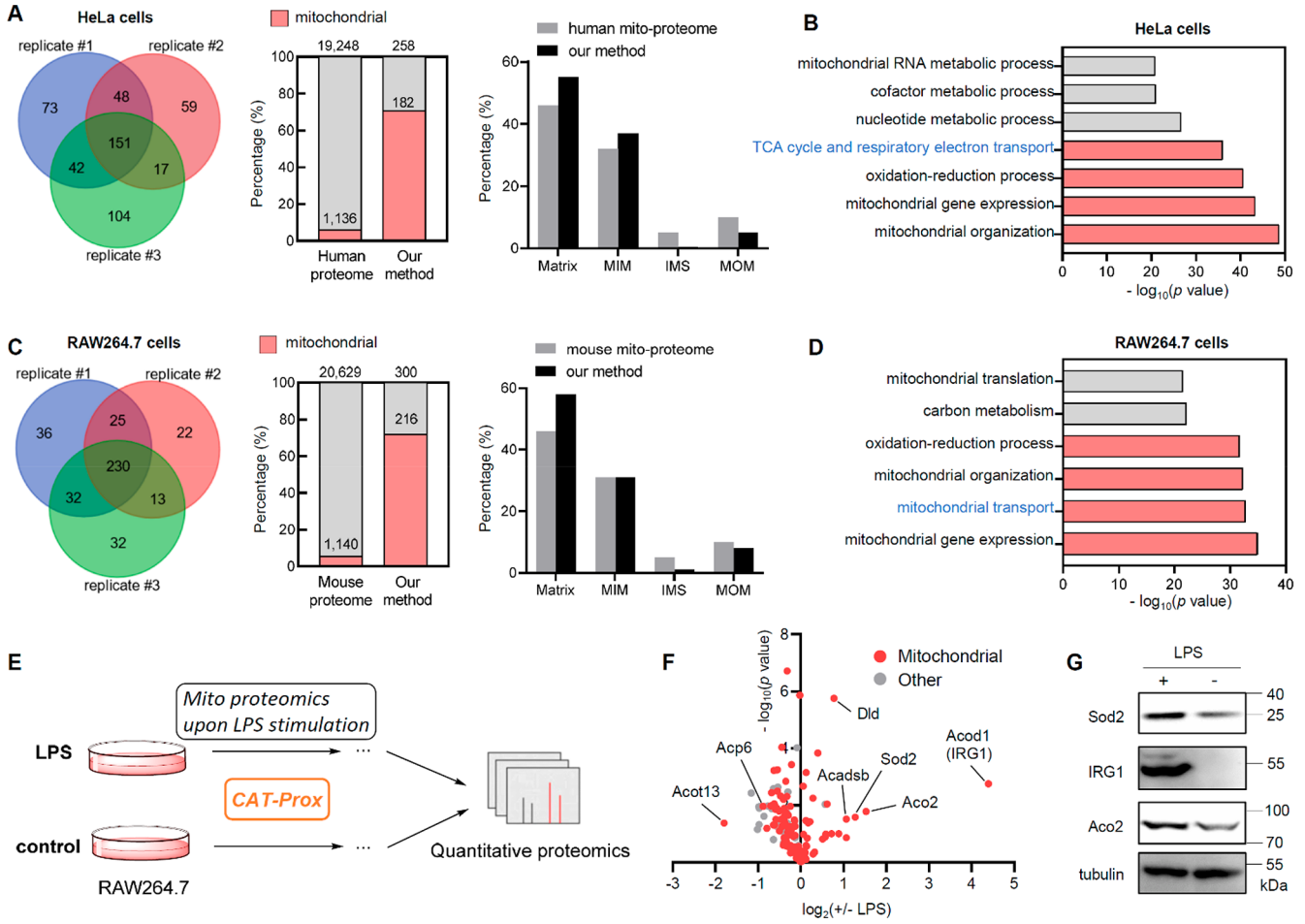

Figure 3. CAT-Prox-enabled profiling of mitochondria proteome and dynamics in living cells. (A) Coupling CAT-Prox with mass spectrometry to identify the labeled subcellular proteome of HeLa cells; 182 mitochondrial proteins were identified from 258 enriched proteins according to the MitoCarta3.0 database (70.5% specificity). Proteins identified as mitochondrial proteins were classified into 'matrix', 'mitochondrial inner membrane (MIM)', 'intermembrane space (IMS)', and 'mithochondrial outer membrane (MOM)'. (B) Gene ontology analysis (Biological Processes) for identified protein from HeLa cells. (C) Protein identification in RAW264.7 cells; 216 mitochondrial proteins from 300 enriched proteins were identified (72% specificity). (D) Gene ontology analysis of the identified proteins from RAW264.7 cells. (E) Combination of CAT-Prox with quantitative protein mass spectrometry analysis based on isotopic dimethyl labeling to dissect the mitochondria proteome dynamics during the inflammatory process of LPS stimulated RAW264.7 cells. (F) Volcano blot showing the regulation of mitochondrial proteins in the inflammatory process of RAW264.7 cells. (G) Immunoblotting analysis of the representative proteins identified above.

phage cells (Figures 3c and S7b). Gene ontology analysis revealed that proteins related with mitochondrial transport were particularly detected in RAW264.7 macrophage cells, likely due to the rapid transportation of metabolites (e.g., citrate, glutamine) that are essential for immunity maintenance (Figure 3d).[25] The proteome difference between HeLa and RAW264.7 cells reflected the correlation between mitochondrial proteomes and cell functions.

Since macrophage inflammatory responses play crucial roles during processes such as bacterial infection and inflammatory diseases,[27] we hope to examine the mitochondria proteome dynamics upon the inflammatory response of macrophages. CAT-Prox was conducted with the LPS-stimulated RAW264.7 cells, and the enriched proteins were analyzed by quantitative mass spectrometry based on isotopic dimethyl labeling with normal RAW264.7 cells as a control (Figures 3e and S8). Upregulation (e.g., IRG1, Aco2, Sod2, Acadsb, and Dld) and downregulation (e.g., Acot13 and Acp6) of mitochondrial proteins were detected in inflammatory responses (Figure 3f). We chose the top three upregulated proteins (IRG1, Aco2, and Sod2) for further immunoblotting analysis. IRG1 was found as the most upregulated protein detected by both CAT-Prox and immunoblotting, indicating the high fidelity of CAT-Prox-based proteomics (Figure 3g). Noteworthy, Aco2 (aconitase 2) and IRG1 (aconitate decarboxylase 1) were responsible for itaconate production in a tandem manner,[28] agreeing with the previous discovery of enhanced itaconate production in LPS-stimulated macrophages.[29,30] Similarly, the increase of reactive electrophile species[29,30] was likely due to the upregulation of Acadsb.[31] The upregulation of the superoxide anion radical scavenger superoxide dismutase [Mn] (Sod2) was probably a self-defense response to the LPS-induced oxidative stress.[32]

CONCLUSION

In summary, we have developed a photocatalytic proteome profiling method (CAT-Prox) with facile spatiotemporal controllability by integrating the unique advantages of photocatalytic decaging chemistry and the protein-reactive quinone methide species, allowing dynamic dissection of mitochondria proteomes of hard-to-transfect cells. The validation of CAT-Prox was shown by mitochondria proteome

https://doi.org/10.1021/jacs.1c09171
J. Am. Chem. Soc. XXXX, XXX, XXX−XXX

profiling of cancer cells as well as macrophage cells. Furthermore, by combining CAT-Prox with quantitative mass spectrometry, we achieved dynamic mitochondrial proteome profiling upon inflammatory stimulation on macrophage cells, which revealed the underlying causes for metabolite change and self-defense during the inflammation response. The advantages of CAT-Prox include the catalytic and *in situ* generation of the reactive labeling probe, avoiding issues from genetic operation, and mislocalization of bait proteins, remote-controllability by light, as well as modular design from the decaging pairs, which enabled CAT-Prox as a general platform for dynamic subcellular proteome profiling in living cells. Expansions of CAT-Prox are straightforward in multiple directions, such as extending to other subcellular organelles by targeting photocatalysts to the desired space, imaging-guided proteomics dissection by taking advantage of the fluorescent property of the photocatalyst, as well as applications to diverse cell types or multicellular settings.

■ ASSOCIATED CONTENT

Supporting Information

The Supporting Information is available free of charge at https://pubs.acs.org/doi/10.1021/jacs.1c09171.

Materials, protocols and data characterizations for all chemical and biological experiments (PDF)

Protein lists from mass spectrometry identification (XLSX)

■ AUTHOR INFORMATION

Corresponding Authors

Xinyuan Fan − *Synthetic and Functional Biomolecules Center, Key Laboratory of Bioorganic Chemistry and Molecular Engineering of Ministry of Education, Beijing National Laboratory for Molecular Sciences, College of Chemistry and Molecular Engineering, Peking University, Beijing 100871, China;* orcid.org/0000-0002-3099-8495; Email: xinyuanfan@pku.edu.cn

Peng R. Chen − *Synthetic and Functional Biomolecules Center, Key Laboratory of Bioorganic Chemistry and Molecular Engineering of Ministry of Education, Beijing National Laboratory for Molecular Sciences, College of Chemistry and Molecular Engineering and Peking-Tsinghua Center for Life Sciences, Peking University, Beijing 100871, China;* orcid.org/0000-0002-0402-7417; Email: pengchen@pku.edu.cn

Authors

Zongyu Huang − *Synthetic and Functional Biomolecules Center, Key Laboratory of Bioorganic Chemistry and Molecular Engineering of Ministry of Education, Beijing National Laboratory for Molecular Sciences, College of Chemistry and Molecular Engineering, Peking University, Beijing 100871, China*

Ziqi Liu − *Synthetic and Functional Biomolecules Center, Key Laboratory of Bioorganic Chemistry and Molecular Engineering of Ministry of Education, Beijing National Laboratory for Molecular Sciences, College of Chemistry and Molecular Engineering, Peking University, Beijing 100871, China;* orcid.org/0000-0003-4109-4245

Xiao Xie − *Synthetic and Functional Biomolecules Center, Key Laboratory of Bioorganic Chemistry and Molecular Engineering of Ministry of Education, Beijing National Laboratory for Molecular Sciences, College of Chemistry and Molecular Engineering, Peking University, Beijing 100871, China*

Ruxin Zeng − *Synthetic and Functional Biomolecules Center, Key Laboratory of Bioorganic Chemistry and Molecular Engineering of Ministry of Education, Beijing National Laboratory for Molecular Sciences, College of Chemistry and Molecular Engineering, Peking University, Beijing 100871, China*

Zujie Chen − *Synthetic and Functional Biomolecules Center, Key Laboratory of Bioorganic Chemistry and Molecular Engineering of Ministry of Education, Beijing National Laboratory for Molecular Sciences, College of Chemistry and Molecular Engineering, Peking University, Beijing 100871, China*

Linghao Kong − *Peking-Tsinghua Center for Life Sciences, Peking University, Beijing 100871, China*

Complete contact information is available at: https://pubs.acs.org/10.1021/jacs.1c09171

Author Contributions

#These authors contributed equally.

Notes

The authors declare no competing financial interest.

■ ACKNOWLEDGMENTS

We acknowledge funding from the Ministry of Science and Technology (2019YFA0904201), the National Natural Science Foundation of China (91957101, 22077004, 21740001, 21937001, 91753000), Beijing Natural Science Foundation (Z200010) and the facility support from the National Center for Protein Sciences at Peking University.

■ REFERENCES

(1) Thul, P. J.; Åkesson, L.; Wiking, M.; Mahdessian, D.; Geladaki, A.; Ait Blal, H.; Alm, T.; Asplund, A.; Björk, L.; Breckels, L. M.; Bäckström, A.; Danielsson, F.; Fagerberg, L.; Fall, J.; Gatto, L.; Gnann, C.; Hober, S.; Hjelmare, M.; Johansson, F.; Lee, S.; Lindskog, C.; Mulder, J.; Mulvey, C. M.; Nilsson, P.; Oksvold, P.; Rockberg, J.; Schutten, R.; Schwenk, J. M.; Sivertsson, Å.; Sjöstedt, E.; Skogs, M.; Stadler, C.; Sullivan, D. P.; Tegel, H.; Winsnes, C.; Zhang, C.; Zwahlen, M.; Mardinoglu, A.; Pontén, F.; von Feilitzen, K.; Lilley, K. S.; Uhlén, M.; Lundberg, E. A subcellular map of the human proteome. *Science* **2017**, *356* (6340), eaal3321.

(2) Christopher, J. A.; Stadler, C.; Martin, C. E.; Morgenstern, M.; Pan, Y.; Betsinger, C. N.; Rattray, D. G.; Mahdessian, D.; Gingras, A.-C.; Warscheid, B.; Lehtiö, J.; Cristea, I. M.; Foster, L. J.; Emili, A.; Lilley, K. S. Subcellular proteomics. *Nat. Rev. Met. Primers* **2021**, *1* (1), 32.

(3) Nunnari, J.; Suomalainen, A. Mitochondria: in sickness and in health. *Cell* **2012**, *148* (6), 1145−59.

(4) Song, J.; Herrmann, J. M.; Becker, T. Quality control of the mitochondrial proteome. *Nat. Rev. Mol. Cell Biol.* **2021**, *22* (1), 54−70.

(5) Singh, A. Subcellular proteome map of human cells. *Nat. Methods* **2021**, *18* (7), 713−713.

(6) Frezza, C.; Cipolat, S.; Scorrano, L. Organelle isolation: functional mitochondria from mouse liver, muscle and cultured filroblasts. *Nat. Protoc.* **2007**, *2* (2), 287−295.

(7) Branon, T. C.; Bosch, J. A.; Sanchez, A. D.; Udeshi, N. D.; Svinkina, T.; Carr, S. A.; Feldman, J. L.; Perrimon, N.; Ting, A. Y. Efficient proximity labeling in living cells and organisms with TurboID. *Nat. Biotechnol.* **2018**, *36* (9), 880−887.

(8) Rhee, H. W.; Zou, P.; Udeshi, N. D.; Martell, J. D.; Mootha, V. K.; Carr, S. A.; Ting, A. Y. Proteomic mapping of mitochondria in

living cells via spatially restricted enzymatic tagging. *Science* **2013**, *339* (6125), 1328−1331.
(9) Yasueda, Y.; Tamura, T.; Fujisawa, A.; Kuwata, K.; Tsukiji, S.; Kiyonaka, S.; Hamachi, I. A Set of Organelle-Localizable Reactive Molecules for Mitochondrial Chemical Proteomics in Living Cells and Brain Tissues. *J. Am. Chem. Soc.* **2016**, *138* (24), 7592−602.
(10) Shiraiwa, K.; Cheng, R.; Nonaka, H.; Tamura, T.; Hamachi, I. Chemical Tools for Endogenous Protein Labeling and Profiling. *Cell Chem. Biol.* **2020**, *27* (8), 970−985.
(11) Geri, J. B.; Oakley, J. V.; Reyes-Robles, T.; Wang, T.; McCarver, S. J.; White, C. H.; Rodriguez-Rivera, F. P.; Parker, D. L.; Hett, E. C.; Fadeyi, O. O.; Oslund, R. C.; MacMillan, D. W. C. Microenvironment mapping via Dexter energy transfer on immune cells. *Science* **2020**, *367* (6482), 1091.
(12) Li, J.; Chen, P. R. Development and application of bond cleavage reactions in bioorthogonal chemistry. *Nat. Chem. Biol.* **2016**, *12* (3), 129−37.
(13) Wang, J.; Wang, X.; Fan, X.; Chen, P. R. Unleashing the Power of Bond Cleavage Chemistry in Living Systems. *ACS Cent. Sci.* **2021**, *7* (6), 929−943.
(14) Chen, Y.; Kamlet, A. S.; Steinman, J. B.; Liu, D. R. A biomolecule-compatible visible-light-induced azide reduction from a DNA-encoded reaction-discovery system. *Nat. Chem.* **2011**, *3* (2), 146−53.
(15) Sadhu, K. K.; Eierhoff, T.; Romer, W.; Winssinger, N. Photoreductive uncaging of fluorophore in response to protein oligomers by templated reaction in vitro and in cellulo. *J. Am. Chem. Soc.* **2012**, *134* (49), 20013−6.
(16) Angerani, S.; Winssinger, N. Visible Light Photoredox Catalysis Using Ruthenium Complexes in Chemical Biology. *Chem. - Eur. J.* **2019**, *25* (27), 6661−6672.
(17) Prier, C. K.; Rankic, D. A.; MacMillan, D. W. Visible light photoredox catalysis with transition metal complexes: applications in organic synthesis. *Chem. Rev.* **2013**, *113* (7), 5322−63.
(18) Fan, X.; Gong, X.; Ma, M.; Wang, R.; Walsh, P. J. Visible light-promoted CO2 fixation with imines to synthesize diaryl alpha-amino acids. *Nat. Commun.* **2018**, *9* (1), 4936.
(19) Zhu, J.; Dai, C.; Ma, M.; Yue, Y.; Fan, X. Visible light-mediated cross-coupling of electrophiles: synthesis of α-amino amides from isocyanates and ketimines. *Org. Chem. Front.* **2021**, *8* (6), 1227−1232.
(20) Weinert, E. E.; Dondi, R.; Colloredo-Melz, S.; Frankenfield, K. N.; Mitchell, C. H.; Freccero, M.; Rokita, S. E. Substituents on Quinone Methides Strongly Modulate Formation and Stability of Their Nucleophilic Adducts. *J. Am. Chem. Soc.* **2006**, *128* (36), 11940−11947.
(21) Liu, J.; Cai, L.; Sun, W.; Cheng, R.; Wang, N.; Jin, L.; Rozovsky, S.; Seiple, I. B.; Wang, L. Photocaged Quinone Methide Crosslinkers for Light-Controlled Chemical Crosslinking of Protein-Protein and Protein-DNA Complexes. *Angew. Chem., Int. Ed.* **2019**, *58* (52), 18839−18843.
(22) Liu, J.; Cheng, R.; Van Eps, N.; Wang, N.; Morizumi, T.; Ou, W.-L.; Klauser, P. C.; Rozovsky, S.; Ernst, O. P.; Wang, L. Genetically Encoded Quinone Methides Enabling Rapid, Site-Specific, and Photocontrolled Protein Modification with Amine Reagents. *J. Am. Chem. Soc.* **2020**, *142* (40), 17057−17068.
(23) Zhou, Y.; Zhou, B.; Pache, L.; Chang, M.; Khodabakhshi, A. H.; Tanaseichuk, O.; Benner, C.; Chanda, S. K. Metascape provides a biologist-oriented resource for the analysis of systems-level datasets. *Nat. Commun.* **2019**, *10* (1), 1523.
(24) Anderson, N. M.; Mucka, P.; Kern, J. G.; Feng, H. The emerging role and targetability of the TCA cycle in cancer metabolism. *Protein Cell* **2018**, *9* (2), 216−237.
(25) Mills, E. L.; Kelly, B.; O'Neill, L. A. J. Mitochondria are the powerhouses of immunity. *Nat. Immunol.* **2017**, *18* (5), 488−498.
(26) Jiang, W.; Reich, I. C.; Pisetsky, D. S. Mechanisms of activation of the RAW264.7 macrophage cell line by transfected mammalian DNA. *Cell. Immunol.* **2004**, *229* (1), 31−40.
(27) Medzhitov, R. Origin and physiological roles of inflammation. *Nature* **2008**, *454* (7203), 428−435.
(28) Wang, Y.; Li, N.; Zhang, X.; Horng, T. Mitochondrial metabolism regulates macrophage biology. *J. Biol. Chem.* **2021**, *297* (1), 100904.
(29) Lampropoulou, V.; Sergushichev, A.; Bambouskova, M.; Nair, S.; Vincent, E. E.; Loginicheva, E.; Cervantes-Barragan, L.; Ma, X.; Huang, S. C.-C.; Griss, T.; Weinheimer, C. J.; Khader, S.; Randolph, G. J.; Pearce, E. J.; Jones, R. G.; Diwan, A.; Diamond, M. S.; Artyomov, M. N. Itaconate Links Inhibition of Succinate Dehydrogenase with Macrophage Metabolic Remodeling and Regulation of Inflammation. *Cell Metab.* **2016**, *24* (1), 158−166.
(30) Timblin, G. A.; Tharp, K. M.; Ford, B.; Winchester, J. M.; Wang, J.; Zhu, S.; Khan, R. I.; Louie, S. K.; Iavarone, A. T.; ten Hoeve, J.; Nomura, D. K.; Stahl, A.; Saijo, K. Mitohormesis reprogrammes macrophage metabolism to enforce tolerance. *Nat. Metab.* **2021**, *3* (5), 618−635.
(31) Farmer, E. E.; Davoine, C. Reactive electrophile species. *Curr. Opin. Plant Biol.* **2007**, *10* (4), 380−386.
(32) West, A. P.; Brodsky, I. E.; Rahner, C.; Woo, D. K.; Erdjument-Bromage, H.; Tempst, P.; Walsh, M. C.; Choi, Y.; Shadel, G. S.; Ghosh, S. TLR signalling augments macrophage bactericidal activity through mitochondrial ROS. *Nature* **2011**, *472* (7344), 476−480.

https://doi.org/10.1021/jacs.1c09171
J. Am. Chem. Soc. XXXX, XXX, XXX−XXX